Defence Science Journal, Vol. 74, No. 6, November 2024, pp. 921-928, DOI : 10.14429/dsj.74.19923

Development of Plenoptic Camera as Wavefront Sensor

Snehal Tonpe[#,*], J. Sreekantha Reddy[#], Chayan Bhar[$], Amit Pratap[#] and Jagannath Nayak[#]

[#]DRDO-Center for High Energy Systems and Sciences, Hyderabad - 500 069, India
[$]Electronics and Communication Engineering, NIT, Warangal - 506 004, India
[*]E-mail: sv721067@student.nitw.ac.in

ABSTRACT

In the field of directed energy systems and remote sensing, it is necessary to carry out the information over a long range. The image signal carrying information reduces its information with increased distance and turbulence level. Due to the optical effects in turbulent atmospheric conditions for distances beyond the range of a kilometer, weak energy signals limit the range for the applications of directed energy systems and remote sensing. The optical effect arises from the temperature variation and causes fluctuations in the refractive index of air. These weak signals have distorted phase and amplitude. Distortions are corrected using Adaptive Optics (AO). The AO uses a wavefront sensor to detect and compensate for the distortion effects. The evaluation of a plenoptic camera into a wavefront sensor is a significant development in the field of AO. A plenoptic camera is efficient for wavefront sensing. In this paper, we develop a plenoptic camera as an alternative to the conventional wavefront sensor to mitigate the effect of strong atmospheric turbulence. Later, we compare the performance of the plenoptic camera with the Shark-Hartmann wavefront sensor. We compare parameters like sensitivity and dynamic range to estimate the minimum and maximum tilt for the captured laser beam under the effect of turbulence. For comparison between wavefront sensors, the image sensor of the same resolution was selected. Experiments were conducted under the same turbulence conditions to record the effect of turbulence on both sensors simultaneously. Our experimental results show that a plenoptic camera gives a less distorted image than a conventional wavefront sensor. The developed plenoptic camera was illustrated to improve over the drawbacks of a conventional wavefront sensor that works well only at weak atmospheric turbulent conditions. Our results show that the developed plenoptic camera gives 40 % greater gradient samples and approximately a divergence of 50 % centroid tilt variation compared to the Shark-Hartmann wavefront sensor. Therefore, a plenoptic camera can be used as a wavefront sensor for strong atmospheric turbulent conditions.

Keywords: Adaptive optics; Plenoptic camera; Wavefront sensor; Micro lens array.

NOMENCLATURE

u,v	: Spherical coordinates
λ	: Wavelength
t	: Time
x,y	: Cartesian coordinates.
f	: The focal length of Micro Lens Array (MLA)
d	: Diameter of the MLA
U	: Distance between the target and the main lens
V	: Distance between the main lens and its image plane.
W	: Distance between the image plane of the main lens and the MLA
Z	: Distance between the sensor and the MLA
F	: The focal length of the main lens
D	: Diameter of the main lens
H	: Size of the target
p	: Pixel size
s	: Sensor width
G	: Gradient samples

1. INTRODUCTION

In the field of adaptive optics, imaging under strong atmospheric turbulence is a challenging job. When a laser beam is propagated in deep atmospheric turbulence, its phase and amplitude get distorted due to irregularities in the refractive index of the air Nurdan[1]. Random variation in the refractive index creates distorted light rays, which significantly affects imaging and beam propagation. As a result, problems like fluctuation in signal intensity, beam wandering from the centroid, and beam breakup come into the picture Larry[2], *et al*. Fluctuation and wandering of the beam are avoided using an aperture of large dimensions. Beam breakup is referred to as the decadence of the spatial coherence of the beam in its transverse plane, which varies from point to point by Vorontsov[3], *et al*. To overcome these problems, wavefront sensors are used.

The wavefront sensor is the optical system that gives information about the wavefront of an incident beam. Wavefront sensors like interferometers and curvature sensors fail to reconstruct wavefront Wu[4], *et al.* Light rays flowing in all three dimensions' directions are known as light fields. Images captured with a light field camera are adjustable for different focal depths Kim[5], *et al*. Significant achievements such as capturing unique information, refocusing, etc. have illustrated that the light field imaging principles are capable of acquiring more information compared to the conventional wavefront sensors.

Received : 20 February 2024, Revised : 25 August 2024
Accepted : 03 September 2024, Online published : 25 November 2024

The Shack-Hartmann wavefront sensor has applications in the field of adaptive optics for defence applications. Porwal[43] developed Shack-Hartmann sensor and discussed its abilities. Defence applications require fast and accurate wavefront sensors Miao[6], *et al.* The Shack-Hartmann sensor acts as a fast wavefront sensor to sense the aberration and wavefront error by measuring the turbulence variance and tilt Dixit[7], *et al.,* Porawal[8], *et al. and* Mishra[9], *et al.* The other applications of the Shack-Hartmann wavefront sensor is in the field of astronomy, for measuring weak turbulence distortion Lawrence[10], *et al.* and Fried[11], *et al.*

Shack-Hartmann wavefront sensor was used in ophthalmology for estimation of higher order aberration in human eyes by Jesson[41] in 2004. Later in 2015 Alameryeen[40] corrected the higher order abreactions using Lytro Illum camera. Lytro Illum is a first implementation of the plenoptic camera also called as plenoptic 1.0. It gives good contrast images at low and higher order of aberrations. *Jesson[13]* proved that it is possible to correct abrerrated images using plenoptic 1.0 camera without using other wavefront sensor and adaptive optics setup. Hence it is said that plenoptic 1.0 camera reduces the complexity, size, weight and cost of the devices compared to AO system use for aberration compensation. Plenoptic 1.0 camera gives single image as single pixel corresponds to one MLA. Plenoptic 1.0 has spatio-angular trade off and fails to extract turbulence details due to two major reasons, (i) It works well only in ideal turbulence conditions, making it impractical (ii) It cannot sense a coherent laser beam for passive imaging techniques using the light field camera. These shortcomings are overcome by a modifying camera design of the plenoptic 1.0 and named it as plenoptic 2.0 which can directly analyse the distorted laser beam. The plenoptic 2.0 camera gives multiple images in single frame that means each MLA captures single image using multiple number of pixels. In this paper use developed the plenoptic 2.0 camera. Further sections discuss in detail about our developed plenoptic camera.

Another type of wavfront sensor is Holographic wavefront sensor. Pathak[42] proposed the algorithm that can detect the holographical introduced unknown wave fronts more accurately. They replace Shack-Hartmann wavefront senor with Holographic wavefront sensor to overcome the limitation of Shack-Hartmann wavefront sensor like low bandwidth and sensitivity at strong turbulence conditions.

The plenoptic camera maps the light field into four-dimensional spaces Landy[13], *et al*. CAFADIS is a plenoptic camera designed based on light field principles that have been proposed and demonstrated by Rodríguez[14], *et al*. to analyze the atmospheric turbulence effect on celestial objects. To analyze the atmospheric turbulence effect on celestial objects. A plenoptic camera mitigates deep atmospheric turbulence effects by Liz[15], *et al*. The plenoptic camera is formed by placing an MLA in a normal camera. The plenoptic camera captures information about the 2-dimensional location of incident light rays and the two-dimensional direction of incidence on the sensor by Landy[13], *et al* and Ng[16], *et al*. Therefore, the final image captured using a plenoptic camera has four dimensions. It is possible to refocus the image after the acquisition, as the plenoptic camera captures the light beam but not the pixels. In single frame plenoptic camera images the target with different angles. The major difference between both the sensors is that the Shack-Hartmann wavefront detects the wavefront of one-point object whereas a plenoptic camera's field of view has multiple object points Yan[17].

The use of a plenoptic camera in smartphones and tablets has attracted its customer base. The robust hardware design makes the plenoptic camera useful for measuring and investing the combustion behavior of fuel particles of aircraft. Lingenauber[22], *et al.* It is also used as a hand lens imager for missions like planetary exploration missions Dong[23], *et al.* for studying rock layers, minerals, and dust. For applications like mobile robotics navigation, it gives higher accurate results and very less processing time (1000 times less than a monocular high definition camera) Huang[24], *et al*. The plenoptic camera is also used for underwater object detection *Yan[17]*. The plenoptic camera is used in many fields as discussed therefore, it is said that the plenoptic camera is cost-effective with low maintenance and gives optimal solutions hence, preferred for many applications.

Designing the plenoptic camera with minimum aberration is a challenging job. This paper contributes to a detailed study of the light field and its optical properties to design the plenoptic camera as a wavefront sensor. The design of our plenoptic camera as a wavefront sensor captures the intensities and direction of light rays. To the best of our knowledge, this is the first one developed in India. Our developed plenoptic camera also has a various application in the field of object recognition, medical imaging, remote sensing, directed energy, museology, industrial inspection, automotive, filmmakers and photographers, Astronomy / solar observation microscopy, imaging pyrometer, etc by Levoy[18], *et al.,* Bedard[19], *et al.,* Debise[20], *et al.* and free space optical communication Noelia[21], *et al.*

The research paper is arranged as follows. Section 2, discusses the related work done in the fields of plenoptic imaging. Section 3 describes the theory of the Shack-Hartman wavefront sensor along with a plenoptic camera with geometry and ray tracing for capturing the images. Section 4 includes the methodology followed to design the plenoptic camera and its image formation process is discussed in detail. Section 5 displays the results and section 6 represents the conclusion followed by future work.

2. LITERATURE REVIEW

The idea of integral imaging was developed by Lippmann in 1908 by Levoy[25], *et al*. Further, for a stereoscopic display, they used several small lenses to form an image with slightly different viewpoints. As a result, it was possible to capture sub-images together with a stereoscopic view, and it was understood that Lippmann's technique can save light field sampling but still unaware of the image formation process. Practically, it is very difficult to create an array of lenses. Therefore, in 1930 Herbert Ives modified Lippmann's idea by using the main lens with a large diameter by Navarro[26], *et al*. He concluded that this technique is pseudoscopic, but not stereoscopic. Later, after a few decades, Chutjian and Collier developed integral imagery Chutjian[27], *et al*. Adelson and Bergen by Adelson[28], *et al.*

brought the concept of the plenoptic function. It is represented using five dimensions, angle, wavelength, time, and position. Adelson and Wang worked on finding the depth of the objects. They used a main lens and pinhole array position before the sensor. Sub-images obtained correspond to slightly different viewpoints by Adelson[28], *et al.* and they named it "Plenoptic Camera". It signified that the camera array captures the light field of an object by Adelson[28], *et al.* and the "lightfield" was expressed as a simplified plenoptic function. The first hand-held plenoptic imaging system was designed in 2005 by Ng[16], *et al.* based on the idea proposed by Adelson and Wang. In 2006 Georgiev and Lumsdaine[30] developed a plenoptic camera using a CCD sensor with increased spatial resolution. It is possible to refocus captured images, which is a major advantage of this developed plenoptic camera by Adelson[29], *et al*.

3. THEORY

3.1 Shack Hartmann Wavefront Sensor

Figures 1a and 1b, represent the conventional wavefront sensor and its spot formation for plane and distorted wavefront. The Shack-Hartman wavefront consists of MLA and the image sensor. An incident beam is projected on each MLA to form an image. The image formed on the focal plane of each MLA determines the liability of the Shack-Hartmann sensor. The reference position is the original centroid position of the beam formed in absence of turbulence, i.e., for the plane wavefront, the reference position is exactly at the center of the MLA as shown in Fig. 1(a). For a distorted wavefront, the laser beam forms its spot with slight displacement as shown in Fig. 1(b). In other words, in the absence of turbulence, there are no distortions and tilt for the acquired image. Whereas, under turbulent conditions, the wavefront gets distorted and the

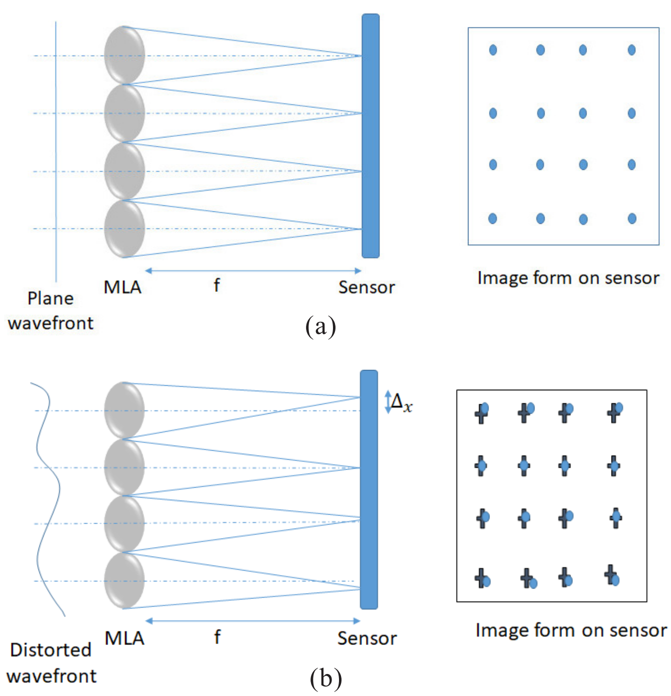

Figure 1. (a) Schematic of Shack Hartmann wavefront sensor under plane wavefront; and (b) Representation of Shack Hartmann Wavefront sensor for distorted wavefront.

image formed on the image sensor is distorted with variation from centroid and experiences the tilt.

The Shack-Hartmann sensor calculates the intensity-weighted gradient of a wavefront over the spatial location of each MLA sub-aperture by LiZ[15], *et al*. For the weak turbulence effect, the centroid tilt and the intensity-weighted average gradient over the sub-aperture remain the same Xiandong[31]. Unfortunately, in the case of strong turbulence conditions, the C-tilt anisoplanatism effect leads to the extraction of inaccurate wavefront information. Effects like scintillation, beam wander, and beam break-up are observed at medium and strong turbulence conditions. In beam wander, parts of the beam get overlapped, which shows various focal points instead of one, and the local gradient is obscure. The focus shift of each MLA should have a certain level of accuracy because if any of the cell images fails to prove focus, the sensor fails to reconstruct the wavefront by Xiandong[31], *et al.* In other words, the Shack Hartmann sensor fails to get sub-aperture images for complex geometric patterns. This is because the sub-aperture images captured using the Shack-Hartmann sensor measure the intensity-weighted average of the phase function.

Many other advanced algorithms by Miao[6], *et al.,* Dixit[7], *et al.,* Mishra[39]*, and* Wu[32], *et al.* are implemented for wavefront reconstruction, but these algorithms cannot change the fundamental design of the Shack-Hartmann sensor. Therefore, the Shack-Hartmann wavefront sensor has its limitations and works well only under weak turbulence conditions. Here, a plenoptic camera as a wavefront sensor comes into the picture. The plenoptic camera traces the dynamic changes in the phase and amplitude of the indented coherent beam. Further sections discuss in detail about the efficiency of a plenoptic camera as a wavefront sensor under deep atmospheric turbulence.

3.2 The Plenoptic Function

The plenoptic function explains the distribution of light rays in volume by Adelson[28], *et al.* It is a seven-dimensional function represented as, $P(u,v,\lambda,t,x,y)$ by Adelson[28], *et al.,* where (u,v) is the angular coordinates. for light rays, λ represents the wavelength, t is the time and the light rays pass through spatial coordinates (x,y,z). The above plenoptic function is reduced by making the following assumptions by Levoy[33], *et al.:*

- Angular coordinates (u,v) are replaced by Cartesian coordinates. (u,v).
- λ is omitted as light is monochromatic,
- Time t is constant, as the function does not vary with time.
- z from spatial resolution is reducible a radiance is constant for long range.

The reduced plenoptic function is four-dimensional called "lumigraph" by Gortler[34], *et al.* and by Michels[34], *et al.* and is represented as, $L(u,v,x,y)$ shown in Fig. 2. The light rays travel from the first plane with coordinates (u,v) and intersect with the second plane at (x,y) coordinates. Coordinates (u,v) and (x,y) specifies the location and direction respectively for the ray. The plenoptic camera can differentiate light rays from all feasible directions and hence comes up with the incoming light field sampling. The light field gives detail about the distribution of the light in volume, with its spatial and angular coordinates by Georgiev[36], *et al.*

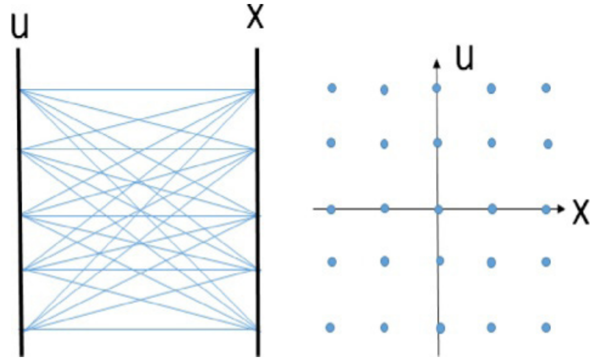

Figure 2. Two plane parameterizing of the light field.

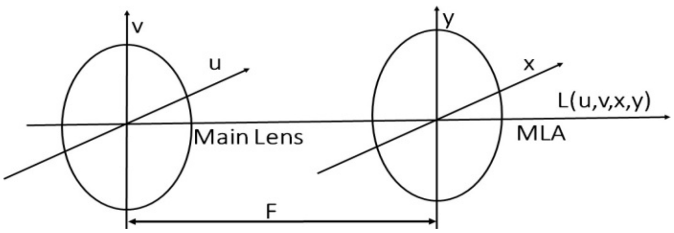

Figure 3. Ray space representation of the light field.

In the matter of a plenoptic camera, the light field originates from the main lens aperture. Figure 3 is a ray space representation of the light field with a single coordinate in each plane for ease of understanding. Consider light rays, i.e. spatial axis x versus direction axis as shown in F. Figure 3 Georgiev[36], *et al.* The light rays originate from a bundle of uniformly spaced to another bundle.

Porwal[43] developed Shack-Hartmann wave front sensor. Table 1. gives comparison between two Shack-Hartmann wavefront sensors, one developed by Porwal[43] and other by Thorlabs[44]. Both the sensors are used for same spectral range but have different specifications with different MLA size, focal length, image sensor, fill factor, etc. Therefore, both the wavefront sensors gives very different tilt range and accuracy values. Thorlabs[44] has tilt range of ± 10mrad with tilt accuracy of 0.01 μ rad, fastest frame rate of 1120 frames per seconds and 15 terms of Zernike terms. Hence, we compared results of our plenoptic wavefront sensor with Shack-Hartmann Sensor developed by Thorlabs[44].

Table I. Comparison between different Shack-Hartmann sensors

	Wavefront Sensor [43]	**WFS20-14AR [44]**
Spectral range	Vis	400 nm - 900 nm
Sampling	16x16	23 x 17
Tilt accuracy	1.78 μ rad.	0.01 μ rad.
Tilt range	± 4mrad	± 10mrad
Fastness	>1000fps	1120fps
Zernike terms	10 terms	15 terms
Pitch	144 μm	300 μm
CMOS sensor	10.6 μm, 256x256, 2200 fps	5μm, 1440 x 1080, 2000 fps
Focal length	8.2 mm	14.6 mm
Fill factor `	87 %	96.7 %

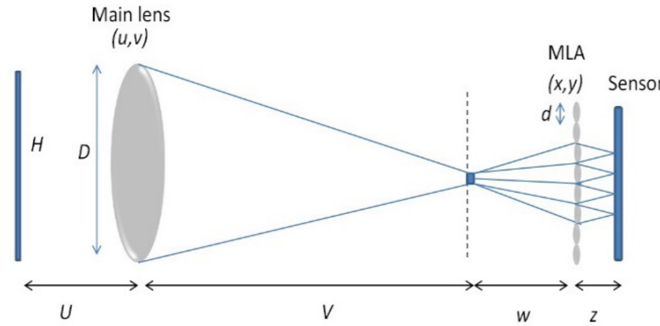

Figure 4. Schematic of Plenoptic camera.

4. PLENOPTIC CAMERA DESIGN

We followed a few considerations for designing the plenoptic camera. These points are:

The focal length (F) selection of main the lens is done using Eqn. (1)

$$\frac{1}{F}=\frac{1}{U}+\frac{1}{V} \tag{1}$$

The distance between the target and the main lens is donated by U. The image plane of the main lens is formed at a distance V from the main lens and z is the distance between MLA and sensor.

The sharpest microlens image is captured by the implementation of Eqn. (2)

$$z=f \tag{2}$$

The light rays from the target fall on the main lens and form an image plane somewhere in between the main lens and the MLA by Prewass[37], *et al*.

The F-number of both the main lens and MLA should be equal to avoid overlapping of images on the sensor plane. The f-number is calculated as:

$$f-number=\frac{focal\,length}{diameter} \tag{3}$$

Figure 4 displays the plenoptic camera ray tracing for the complete wavefront reconstruction. The plenoptic camera captures information, as the light rays travel from the target towards the main lens (u,v) plane. The image plane of the main lens is indented in front of the MLA plane (x,y). The images formed on each micro lens are further captured and recorded on the sensor. In other words, each microlens forms the array of images on the sensor. This micro image gives specific (u,v) information related with it and other (x,y) information for each pixel.

Their idea, to place the MLA after the image plane of the main lens, proved significant in get better spatial resolution. The dissimilar angular components getting split by the Fourier transform of the main lens. Therefore, interference issues are absent for the wavefront sensed with sub-apertures of the plenoptic camera. The image sensor provides information about the intensity and the direction of light as it receives light from all MLA at different positions. Since the MLA focuses at infinity, an individual pixel in a sub-aperture image corresponds to a specific angle for entering light rays by Horn[38], *et al*. The light rays diverge from the MLA at a different location on the sensor and provide a directional resolution of an object.

Silent features of our developed plenoptic camera are as follows:

- The hardware design enables to give reconstructed wavefront. This is because, the Fourier transforms of main lens automatically separates the different angular components. Therefore, interference issues are absent at sub-aperture images
- The plenoptic camera acquires more information than conventional wavefront sensors.

5. RESULTS

Plenoptic camera calibration is necessary to get precise data. The calibration procedure includes the determination of the main lens and the MLA parameters. The distance between the MLA and the sensor is set such that the image sensor covers the total number of MLA. The center point of each MLA is aligned such that is image is formed at the center of the MLA. The focus adjustment depends on the target distance. Initial calibration of the plenoptic camera is sufficient to image the target.

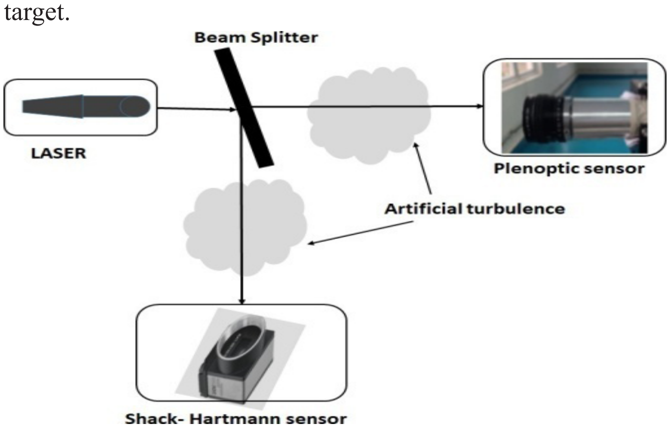

Figure 5. Lab level set up for comparison of Shack-Hartmann and Plenoptic camera.

We have designed and calibrated the plenoptic camera. Based on the theory discussed in this paper for imaging under turbulent conditions and benchmarked its characteristics against wavefront sensor and compared its characteristics with conventional wavefront sensor. We have successfully imaged and tested the performance of our plenoptic camera up to a range of 5 kilometers under turbulent conditions for object detection. To check the efficiency of the plenoptic camera as a wavefront sensor, indoor experiments were conducted by generating artificial turbulence. Artificial turbulence was generated at the lab level by blowing hot and cold air in the path towards the source. We captured the images for both the sensors simultaneously to compare the effect of wavefront distortions under the effect of turbulence. Figure 5 represents our lab-level setup. The MLA has a pitch size of 250 microns. The focal length of MLA is selected in such a way that both of the MLA and the main lens has same f-number. We used Shack-Hartmann sensor designed by Thorlabs with a pitch size of 300 microns.

The image sensor used for both Shack-Hartmann and plenoptic camera has a pixel size of 5 microns and an image sensor resolution of 1440*1080 as shown in Table 2.

Table 2. Parameter comparison performance between conventional wavefront sensor and the plenoptic camera

	Shack-Hartmann	Plenoptic camera
MLA Pitch (μm)	300	250
Pixel Size (μm)	5	5
Sensor resolution	1440*1080	1440*1080

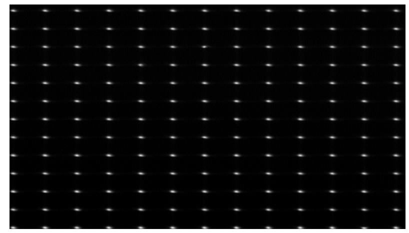

Figure 6. Image captured under normal condition.

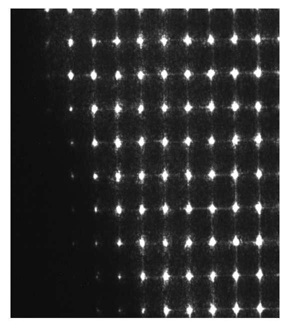

Figure 7. Image captured using the Shack-Hartmann sensor under turbulence.

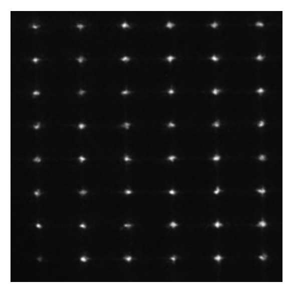

Figure 8. Image captured using the Plenoptic Sensor under turbulence.

Image acquired under normal conditions (without turbulence) has zero distortion as shown in Figure 6. In this condition, the beam spot is formed exactly at the centre of the MLA. Figure 7 and Fig. 8 display the image acquired using the Shack-Hartmann wavefront sensor and plenoptic camera respectively under strong turbulent conditions. It was observed that the image captured using the Shack-Hartmann sensor has interference effects as explained in Fig. 1(b). Figure 7 shows the captured turbulence effects and beam distortions. Whereas, the Fig. 8 is the image captured by the plenoptic camera, is at the centre of MLA with lesser tilt and distortions compared to the conventional wavefront sensor. Therefore from Fig. 8, we can say that the plenoptic camera preserves the full wavefront information for future analysis and computations. The image formed on each MLA of the plenoptic camera is due to the turbulence effect, the laser beam incident on the sensor gets scattered.

The wavefront camera should be properly designed to match the operating conditions and verify parameters like the sensitivity and the dynamic range. Sensitivity for wavefront sensor defines the minimum displacement of the centroid position concerning the reference position. The dynamic range calculates the magnitude of maximum wavefront aberrations. In other words, it gives the values of maximum displacement of centroid position. We quantify the values of minimum and maximum tilt to illustrate the change in the available gradient information.

Change in centroid positions gives information of the turbulence effect. The shifted centroid from the optical axis of each sub-aperture is predicted by calculating wavefront tilt as shown by equations as follows.

$$\left(\Delta_x,\Delta_y\right)_{\min}=\frac{p}{f} \tag{4}$$

$$\left(\Delta_x,\Delta_y\right)_{\max}=\left(\Delta_x,\Delta_y\right)_{\min}*\frac{d}{2p} \tag{5}$$

$$G=\left(\frac{w}{d}\right)^2 \tag{6}$$

For the plenoptic camera, minimum and maximum tilt is calculated using the below equations by Wu[32], *et al*.

$$\left(\Delta_x,\Delta_y\right)_{\min}=\frac{d}{F} \tag{7}$$

$$\left(\Delta_x,\Delta_y\right)_{\max}=\frac{w}{2f} \tag{8}$$

$$G=\left(\frac{d}{p}\right)^2 \tag{9}$$

Table 3 results give insight into the changes in the obtainable gradient information derived from the same MLA between both wave front sensors. We compared the minimum wavefront tilt $(\Delta_x, \Delta_y)_{\min}$, maximum $(\Delta_x, \Delta_y)_{\max}$ along with the minimum gradient sample size of the Shack-Hartmann sensor and the plenoptic camera as shown in Table 3. The minimum wavefront tilt referred to sensitivity is 14 % greater with the plenoptic camera, whereas the maximum wavefront tilt has a difference of 54 %. The Shack-Hartmann sensor produces 60 % fewer gradient samples than the plenoptic camera.

The count of the gradient sample depends dynamically on the wavefront distortion. From the above comparison, it is clear that the plenoptic camera gives better results than the Shack-Hartmann sensor i.e. turbulence effect is compensated using a plenoptic camera, therefore it can be used as a wavefront sensor. The MLA of both the sensor gives the same effect but the major difference between them is principle design of both the sensors that decides the way of sensing the wavefront.

Table 3. Comparison between conventional wavefront sensor and the plenoptic camera

	Shack-Hartmann	Plenoptic camera
Min. tilt (mrad)	0.3424	0.294
Max. tilt (mrad)	10.26	4.70
Gradient samples	711	2065

7. CONCLUSIONS

Under strong turbulent conditions, the wavefront frequently faces challenges like zero intensity and coincidence of the light. For the Shack-Hartmann sensor, it is not possible to identify and reconstruct both of these issues. On the other hand, a plenoptic camera easily deals with these challenges of wavefront sensing specifically for severe turbulence conditions. This is because the plenoptic camera is resistant to effects like deep scintillation and self-interference of the distorted wavefront. Our developed plenoptic camera successfully captures four-dimensional information about the light field and estimates more angular information than the conventional Shack-Hartmann sensor. For wavefront reconstruction at high turbulence, the plenoptic camera proved more efficient as compared to other conventional wavefront sensors. Therefore, for applications like directed energy systems and remote sensing, we can use the plenoptic camera for sensing weak to strong turbulence distortions compared to the conventional wavefront sensor.

8. FUTURE WORK

The beam efficiency has a crucial role in the applications of the LASER beam technology. To increase the beam efficiency for long-range mathematical turbulence analysis fails, there is a need to study actual structural turbulence. In the future, we plan to use the developed a plenoptic system and design image reconstruction algorithms for beam corrections under real-time turbulent atmospheric conditions. The post image processing algorithms can be used for image correction, phase and amplitude corrections, and decoding optical signals. Our plenoptic camera has two limitations, first is refocusing distance limits number of pixels responsible for angular information. It can be overcome by modifying the design of plenoptic camera. Second, slope response and accuracy can further improved with the use of deep learning approach

REFERENCES

1. Nurdan, A.B. & Aydin, Y. Wave-front aberrations of laser beams propagating through the atmosphere. *COAT-2019:* Workshop (Communications and Observations through Atmospheric Turbulence: characterization and mitigation), Châtillon, France, Dec 2019. doi:10.34693/COAT2019-S2-001.
2. Larry, A.; Ronald, P.; Richard, S. & Ronald, P. Beam wander effects on the scintillation index of a focused beam. *Int. Soc. Optics and Photonics,* 2005, 28-37. doi:10.1117/12.604855.
3. Mikhail, V.; Jim, R.; Gary, C.; Rao, V.S.; Leonid, B.; Thomas, W.; and Lewis, C. & Lewis R.Jr. Deep turbulence effects compensation experiments with a cascaded adaptive optics system using a 3.63 m telescope. *Applied Optics,* 2009, **48**, A47-A57.

doi:10.1364/AO.48.000A47

4. Wu, C. & Ko, J.C. Determining the phase and amplitude distortion of a wavefront using a plenoptic sensor. *J. Opt. Soc. Am,* 2015, A32, 964-978.
5. Kim, H.M.; Kim, M.S.; Chang, S.; Jeong, J.; Jeon, H.-G. & Song, Y.M. Vari-focal light field camera for extended depth of field. *Micromachines* 2021, **12**, 1453. doi:10.3390/mi12121453
6. Miao, Z.; Markus, V.; Krasimir, A.; Hans-Joachim,G.; Dieter, S.; Robin, S.; Siegmar, W.; Viktor, S. & Jörg, M.A. Novel plenoptic camera-based measurement system for the investigation into flight and combustion behavior of refuse-Derived fuel particles. *ACS Omega,* 2023, **8**(19), 16700-16712. doi: 10.1021/acsomega.2c08004.
7. Porwal, P.; Awakash, D. & Mishra, S. Evaluation of finitely conjugated afocal telescope using SH-WS for adaptive optics, 2014. doi:10.13140/RG.2.1.4011.7446/1.
8. Dixit, A.; Porwal, V.; Kumar, A. & Mishra, S. Systematic characterization of near-index-matched optics based atmospheric turbulence simulator. *MAPAN-J. Metrol. Soc. India,* 2020, **35**, 221–232. doi: 10.1007/s12647-020-00370-9.
9. Porwal, V.; Dixit, A.; Mishra, S.; Kumar, A. & Gupta, A. *In* International Conference on Optics and Photonics. Characterization of atmosphere-like turbulence for the performance evaluation of Adaptive Optics System. 2015. doi: 10.13140/2.1.4493.6489.
10. Lawrence, Robert,S. & John, W.A. Survey of clear air propagation effects relevant to optical communications. *Proceedings of the IEEE*, 1970, **58**, 1523-1545. doi:10.1109/PROC.1970.7977
11. Fried, D.L.; Mevers, G.E. & Keister J.R. Measurements of laser-beam scintillation in the atmosphere. *JOSA57*, 1967, **57**, 787-797.
12. Jose, R.R.; Castelló, E.; Conde, C.; Valido, M. & Marichal, H.J. 2D-FFT implementation on FPGA for wavefront phase recovery from the CAFADIS camera. *Proc SPIE*, 2008, 7015. doi:10.1117/12.789312.
13. Landy, M. & Movshon, J. The plenoptic function and the elements of early vision. *Comput. Models of Visual Process.*, 1991, 3-20.
14. Jose, R.R.; Femenia, B.; Montilla, I.; Rodriguez, R.; Luis, F.; Marichal, H.J.; José; Lüke, J.; López, R.; Díaz, J. & Martin, Y. The CAFADIS camera: A new tomographic wavefront sensor for adaptive optics. *Adaptative Optics for Extremely Large Telescopes,* 2010, 05011. doi:10.1051/ao4elt/201005011.
15. Zhenghan, L. & Xinyang L. Fundamental performance of transverse wind estimator from Shack-Hartmann wavefront sensor measurements. *Opt. Express*, 2018, **26**(9), 11859-11876. doi:10.1364/OE.26.011859.PMID:29716103.
16. Ng. R; Levoy, M; Bredif, M.; Duval, G.; Horowitz, M.P. & Design, D. Light field photography with a hand-held Plenoptic camera. *Technol. Rep. CSTR*, 2005.
17. Yan, W.; Quan, S. & Kai, H. Turbulence image correction using focused light field camera. *AIP Advances*, 2024, **14**(6), 065210. doi: 10.1063/5.0197159.
18. Levoy, M.; Ng, R.; Adams, A.; Footer, M. & Horowitz, M. Light field microscopy, *ACM Trans. Graph*, 2006. **25**(3), 924.
19. Bedard, N.; Shope, T.; Hoberman, A.; Haralam, M.; Shaikh, N.; Kovacevic, N.; Balram, J. & Tosic, N. Light field potoscope design for 3D in vivo imaging of the middle ear. *Biomed. Opt. Express,* 2017*,* **8**(1), 260–272. doi:10.1364/BOE.8.000260.
20. Debise, M. & Ihrke, L. Light field microscopy with a consumer light-field camera 3D Vis. *In* 2015 International Conference on 3D Vision, Lyon, France, 2015, 335–343. doi:10.1109/3DV.2015.45.
21. Noelia, M.; Luis, R.; Angel, A.; Iciar. M. & Joan, T. Plenoptic wavefront sensor for free-space optical communications. *Proc. SPIE 11993,* Free-Space Laser Communications XXXIV, 2022. doi: 10.1117/12.2607320
22. Lingenauber, M.; Fröhlich, F.A.; Krutz, U.; Nisler, C. & Strobl, K.H. In-Situ Close-Range Imaging with Plenoptic Cameras. IEEE Aerospace Conference, Big Sky, MT, USA, 2019, 1-16. doi: 10.1109/AERO.2019.8741956.
23. Dong, F.; Ieng, S.H.; Savatier, X.; Etienne-Cummings, R. & Benosman, R. Plenoptic cameras in real-time robotics. *Int. J. Robotics Res.*, 2013, **32**, 206–217. doi:10.1177/0278364912469420.
24. Huang, J.; Yao, L.; Wu, S. & Wang, G. Wavefront reconstruction of shack-hartmann with under-sampling of sub-apertures. *Photonics,* 2023, **10**, 65. doi: 10.3390/photonics10010065
25. Levoy, M. Light fields and computational imaging. *Computer (Long.Beach.Calif),* 2006*,* **39**, 46- 55. doi:10.1109/MC.2006.270.
26. Naro, H.; Dorado, A.; Genaro, S. & Manuel, M.C. Three dimensional imaging and display through integral photography. *J. Inf. Commun. Convergence Engine.*, 2014, **12**, 89-96. doi:10.6109/jicce.2014.12.2.089.
27. Chutjian, A. & Collier, R. Recording and reconstructing three-dimensional images of computer-generated subjects by Lippmann integral photography. *Appl. Optics*, 1968, **7**, 99-103. doi:10.1364/AO.7.000099.
28. Adelson, E.H. & Bergen, J.R. The Plenoptic function and the elements of early vision. *Comput. Models of Visual Process. MIT*, 1991, 3–20.
29. Adelson, E.H. & Wang, A. Single lens stereo with a Plenoptic camera. *IEEE Transact. Pattern Analysis and Mach. Intell.*, 1992, **14**(2), 99-106. doi:10.1109/34.121783.
30. Lumsdaine, A. & Georgiev, T. The focused Plenoptic camera. Proceedings of IEEE International Conference on Computational Photography, 2009, 1-8. doi:10.1109/ICCPHOT.2009.5559008

31. Xiandong, S. & Bing, D. Performance analysis of plenoptic wavefront sensor. Proc. SPIE 12706, First International Conference on Spatial Atmospheric Marine Environmental Optics, 2023.
doi: 10.1117/12.2683221
32. Wu, C.; Ko, J.; & Davis, C.C. Imaging through water turbulence with a plenoptic sensor. Laser communication and propagation through the atmosphere and oceans, 2016, 9979.
doi:10.1117/12.2239118.
33. Levoy, M. & Hanrahan, P. Light field rendering. Proceedings of SIGGRAPH, ACM, 1996, 31–42.
doi: 10.1145/237170.237199.
34. Gortler, S.J.; Grzeszczuk, R.; Szeliski, R. & Cohen, M. The lumigraph. Prceedings of SIGGRAPH ACM*,* 1996, 43–54.
doi: 10.1145/237170.237200.
35. Michels, T. & Koch, R. Ray tracing-guided design of plenoptic cameras*. In* tern. Conference 3D Vision (3DV)*,* 2021, 1125-1133.
doi: 10.1109/3DV53792.2021.00120.
36. Georgiev, T. & Intwala, C. Light-field camera design for integral view photography. tech.rep. Adobe Systems, 2006.
37. Perwass, C. & Wietzke, L. Single lens 3D-camera with extended depth-of-field*. In* Proc. SPIE, Human vision and electronic imaging XVII*,* 2012, 8291,45-59.
doi:10.1117/12.909882.
38. Horn, B.K. Robot Vision. *MIT,* 1986.
39. Mishra, S.; Porwal, V.; Meena, D.; Dixit, A.; & Mohan, D. & Gupta, A. Testing of fast wavefront sensor for off-axis aberrations.
doi: 10.13140/2.1.1583.4565.
40. Alameryeen, H.; Arines, J. & Acosta, E. Plenoptic cameras for imaging through aberrated systems. 2015, 1-2.
doi: 10.1109/MOC.2015.7416495.
41. Jesson, M.; Pachiyappan, A. & Ganesan, A. higher order aberrations of the eye in a young indian population. 2004, **6**.
42. Pathak, B. & Boruah, B. Improved wavefront reconstruction algorithm for Shack─Hartmann type wavefront sensors. *J. Optics.* 2014, **16**, 10.1088/2040-8978/16/5/055403.
43. Porwal, V.; Dixit, A.; Mamgain, A.; Mishra, S. & Gupta, A. A systematic performance evaluation of indigenously developed Shack-Hartmann wavefront sensor. *Indian J. Pure & Appl. Physics*. 2016, **54**, 419-426.
44. https://www.thorlabs.com/thorproduct.cfm?partnumber=WFS20-14AR,

CONTRIBUTORS

Ms Snehal Tonpe is pursuing PhD in Electronics and communication from NIT, Warangal and working as a Senior Research Fellow at DRDO-CHESS. Her areas of research include: Development of plenoptic imaging system and its image processing algorithms. In the current study: She used the plenoptic camera as the wavefront sensor and compared its performance with the conventional wavefront sensor and presented the results with relevant figures and tables in this paper.

Mr J. Sreekanth Reddy is Scientist F and Group Head at DRDO-CHESS.
In the current study, he computed methodology for plenoptic camera as a wavefront sensor.

Dr Chayan Bhar obtained his PhD in optical networks from IIT, Kharagpur and working as an Assistant professor in ECE department at NIT, Warangal.
In the current study, he contributed for validation, formulation of problem and review the drafts.

Dr AMIT Pratap obtained his PhD from Pantnagar University and working as a Scientist F at DRDO-CHESS.
In the current study he contributed in formal analysis, project administration and resource validation

Dr Jagannath Nayak obtained his PhD in Electrical Communication Engineering from the Indian Institute of Science (IISc), and working as Lab Director at DRDO-CHESS.
In the current study, he supervised and funded this research project.